





## ORIGINAL RESEARCH

# Stimulation of constitutive nitric oxide uniquely and compensatorily regulates intestinal epithelial cell brush border membrane Na absorption

Balasubramanian Palaniappan , Palanikumar Manoharan , Subha Arthur, Soudamani Singh , Usha Murughiyan & Uma Sundaram 

Department of Clinical and Translational Sciences, Joan C Edwards School of Medicine, Marshall University, Huntington, West Virginia

## Keywords

Constitutive nitric oxide, Na homeostasis, sodium glucose cotransport, sodium proton exchange.

## Correspondence

Uma Sundaram, Joan C Edwards School of Medicine, Marshall University, 1600 Medical Center Drive, Huntington, WV 25701.  
Tel: +1 304-691-1841  
Fax: +1 304-691-1840  
E-mail: sundaramu@marshall.edu

## Funding Information

This work was supported by National Institutes of Health grants DK-67420, DK-108054, P20GM121299-01A1 and Veteran's Administration Merit Review grant BX003443-01 to U. Sundaram.

Received: 23 March 2019; Revised: 10 April 2019; Accepted: 12 April 2019

doi: 10.14814/phy2.14086

*Physiol Rep*, 7 (9), 2019, e14086,  
<https://doi.org/10.14814/phy2.14086>

## Abstract

In the mammalian small intestine, sodium is primarily absorbed by  $\text{Na}^+/\text{H}^+$  exchange (NHE3) and Na-glucose cotransport (SGLT1) in the brush border membrane (BBM) of villus cells. However, how enhanced cellular constitutive nitric oxide (cNO) may affect NHE3 and SGLT1 remains unclear. Both in vivo in rabbit intestinal villus cells and in vitro IEC-18 cells, administration of NO donor, GSNAP, modestly increased cNO. GSNAP stimulated SGLT1 in villus and IEC-18 cells. The mechanism of stimulation was secondary to an increase in the affinity of SGLT1 for glucose. The change in SGLT1 was not secondary to altered Na-extruding capacity of the cell since  $\text{Na}^+/\text{K}^+$ -ATPase was decreased by GSNAP treatment. In contrast, GSNAP inhibited NHE3 activity in villus cell BBM. The mechanism of NHE3 inhibition was secondary to reduced BBM transporter numbers. These studies demonstrated that the physiological increase in cNO uniquely regulates mammalian small intestinal NHE3 and SGLT1 to maintain Na homeostasis.

## Introduction

The mammalian small intestine absorbs approximately 7.5 L of water every day, primarily mediated by the absorption of 650 mEq of sodium (Na). The two most important pathways of Na absorption in the small intestine are coupled electroneutral NaCl absorption and nutrient-dependent Na absorption. Coupled NaCl absorption occurs via the dual operation of  $\text{Na}^+/\text{H}^+$  exchange (NHE3) and  $\text{Cl}^-/\text{HCO}_3^-$ -exchange (DRA or PAT-1) located in the brush border membrane (BBM) of

absorptive villus, but not secretory crypt cells. Na-glucose cotransport (SGLT1), also located in the BBM of the villus cells, is the most abundant nutrient-dependent Na absorptive process in the mammalian small intestine (Hoogerwerf et al. 1996; Sundaram et al. 1997; Donowitz et al. 2005; Coon et al. 2007). SGLT1 is not only important for Na absorption, but also for glucose absorption which is the most abundant nutrient in the diet (Wright et al. 2006). In fact, the foundation of oral rehydration therapy is preserved SGLT1, which is the cornerstone of therapy for diarrheal diseases in developing countries.

SGLT1 is a secondary active transport process requiring a favorable transcellular Na gradient which is provided by the Na<sup>+</sup>/K<sup>+</sup>-ATPase located in the basolateral membrane (BLM) of villus cells (Wright *et al.* 2007).

Regulation of SGLT1 and NHE3 by various hormones such as aldosterone and immune inflammatory mediators have been demonstrated (Sundaram *et al.* 1999; De La Horra *et al.* 2001). Furthermore, in an animal model of chronic intestinal inflammation, resembling human inflammatory bowel disease, it was shown that NHE3 was not affected, while SGLT1 and other Na-dependent nutrient cotransport processes were inhibited (Sundaram and West 1997; Sundaram *et al.* 1998a,b; Saha *et al.* 2012).

Nitric oxide (NO) is a highly active molecule shown to regulate multiple gastrointestinal functions. Small amounts of NO (constitutive NO/cNO) regulate normal intestinal physiological processes like motility, blood flow, and mucosal permeability (Shah *et al.* 2004). In contrast, during intestinal inflammation, high levels of NO (inducible NO/iNO) are produced and is thought to be involved in enterocyte apoptosis and necrosis, intestinal barrier failure resulting in bacterial translocation, reduced colonic motility, secretory diarrhea, and pathogenesis of inflammatory bowel disease (Kubes and McCafferty 2000; Grisham *et al.* 2002). Intestinal absorption and secretion has been shown to be affected by cNO (Barry *et al.* 1994; Coon and Sundaram 2003; Coon *et al.* 2005, 2007, 2008; Arthur *et al.* 2014). Nevertheless, many NO-mediated effects on intestinal electrolyte transports are contradictory. For example, in some studies, NO has been shown to enhance electrolyte transport in guinea-pig small intestine, rat jejunum, ileum, colon, and human colon (MacNaughton 1993; Tamai and Gaginella 1993; Stack *et al.* 1996; Mourad *et al.* 2003). However, other studies demonstrated that NO has both proabsorptive and prosecretory roles in cholera toxin-induced secretion, basal proabsorptive tone in the intestine and reversal of L-arginine induced fluid secretion (Schirgi-Degen and Beubler 1998; Turvill *et al.* 1999; Mourad *et al.* 2003).

Additionally, previous *in vivo* and *in vitro* studies have demonstrated that the inhibition of cNO differentially regulates NHE3 and SGLT1 in intestinal epithelial cells (Coon *et al.* 2005, 2007, 2008; Palaniappan and Sundaram 2018). *In vivo* administration of L-Ng-Nitroarginine methylester (L-NAME) to rabbits and *in vitro* administration to IEC-18 cells, reduced cNO by the inhibition of cNO synthase (cNOS). Inhibition of cNO stimulated BBM NHE3 in both *in vivo* and *in vitro* (Coon *et al.* 2007). The mechanism of stimulation of NHE3 was secondary to increased BBM transporter numbers. In contrast, diminished cNO resulted in the inhibition of SGLT1 in rabbit villus cells and IEC-18 cells (Coon *et al.* 2005, 2008). Kinetic and molecular studies demonstrated

that the mechanism of inhibition was secondary to a reduction in the affinity of SGLT1 for glucose. The inhibition of SGLT1 was not secondary to the reduction in the Na-extruding capacity of cells, since Na<sup>+</sup>/K<sup>+</sup>-ATPase was unchanged and the observed effects persisted in BBMV where this is not an issue. In summary, these studies demonstrated that *in vivo* and *in vitro* inhibition of cNO stimulated BBM NHE3, but inhibited SGLT1. Thus, inhibition of cNO differentially regulates NHE3 and SGLT1 in the mammalian small intestine. However, the effect of physiological increases in cNO on these two primary Na absorptive pathways in the mammalian small intestine remains unknown. Thus, it is important to determine the effect of moderate, direct increases in cNO on SGLT1 and NHE3 to fully elucidate the mechanism of physiological changes in cNO on these two important BBM Na absorptive processes.

## Methods

### Ethical approval

New Zealand White male rabbits (2.5–2.7 kg) were obtained from Charles River Laboratories International, Inc., USA. All animal handling, treatments and euthanasia were carried out according to the protocol approved by Marshall University institutional animal care and use committee (IACUC) regulations. Before and throughout the experiments, animals had free access of water and food and were kept in 12 h light–dark cycle room in the animal facility.

### Drug treatment

To induce nitric oxide production in the rabbits, 1 mL of 500 nmol/L N-(β-D-glucopyranosyl)-N2-acetyl-S-nitrosod, L-penicillaminamide (GSNAP; Calbiochem, USA), a conventional NO donor, was injected intramuscularly. Control animals were injected with sterile distilled water. The animals were euthanised with 120 mg/kg of pentobarbital sodium (approved by IACUC) through the ear vein after 24 h of GSNAP treatment.

### Villus cell isolation and BBM vesicle preparation

Villus cells were isolated from the GSNAP treated and control rabbit intestine by a calcium chelation technique as previously described (Sundaram *et al.* 1991, 1997). BBM vesicles (BBMV) from rabbit intestinal villus cells were prepared using divalent cation (Mg<sup>2+</sup>) chelation and differential centrifugation technique as previously reported (Sundaram *et al.* 1997, 1998a). BBMV were

suspended in an appropriate reaction medium for each uptake experiment or with an appropriate buffer for molecular studies.

### Cell culture and treatment

Rat IEC-18 cells were grown in DMEM supplemented with 0.2 U/mL of insulin, 0.5 mmol/L  $\beta$ -hydroxybutyrate and 10% fetal calf serum, and incubated at 37°C with 10% CO<sub>2</sub> in a humidified atmosphere. Cells grown as postconfluent monolayers were used for all the experiments. The cells were treated with 250 nmol/L GSNAP (Calbiochem, USA) for 24 h to increase cNO or with vehicle in control cells prior to the uptake experiments.

### Measurement of NO

Total NO levels were measured in cells (villus and IEC-18) by Griess reaction colorimetric assay (Cayman chemicals, USA) according to the manufacturer's instruction. Briefly, GSNAP treated and untreated villus and IEC-18 cells were lysed with phosphate-buffered saline (PBS) by sonication. The cell lysate was then centrifuged and the clear supernatants were used for the assay to measure total NO (nitrite+nitrate). Samples were read at 540 nm and total NO concentrations were determined with the nitrate standard curve.

### NHE3 uptake studies in IEC-18 cells

Uptake studies for Na<sup>+</sup>/H<sup>+</sup> exchange were performed in confluent IEC-18 cells as described previously (Palaniappan and Sundaram 2018). Briefly, the cells were incubated for 10 min in buffer containing 70 mmol/L TMACl, 50 mmol/L NH<sub>4</sub>Cl, 5 mmol/L KCl, 1 mmol/L MgSO<sub>4</sub>, 2 mmol/L CaCl<sub>2</sub>, 5 mmol/L glucose, 15 mmol/L Tris-HEPES (pH 7.4) and washed with wash buffer containing 120 mmol/L TMACl and 15 mmol/L Tris-HEPES (pH 7.4). Uptake was initiated by incubating the cells for 2 min with a reaction medium containing Na-free buffer with 10  $\mu$ Ci of <sup>22</sup>Na and 1 mmol/L NaCl in the presence or absence of 50  $\mu$ mol/L EIPA (NHE3 inhibitor). The reaction was stopped and the cells were washed twice with ice-cold phosphate-buffered saline. The cells were then incubated with 1 N NaOH for 20 min at 70°C, to digest the cells, before addition of 4 mL of scintillation fluid (Ecoscint; National Diagnostics). Radioactivity was determined in a Beckman 6500 Beta scintillation counter.

### Na-glucose cotransport uptake studies in IEC-18 cells

Na-glucose cotransport uptakes were performed in post-confluent IEC-18 cells using a previously described

protocol (Palaniappan and Sundaram 2018). Briefly, the cells were washed and incubated with Na-free buffer containing 130 mmol/L TMACl, 4.7 mmol/L KCl, 1 mmol/L MgSO<sub>4</sub>, 1.25 mmol/L CaCl<sub>2</sub>, 20 mmol/L HEPES (pH 7.4 at 37°C) for 10 min. Uptake was initiated by incubating the cells for 2 min in a Tris-HEPES (pH 7.4) reaction medium containing 130 mmol/L NaCl, 10  $\mu$ Ci of <sup>3</sup>H-O-methyl glucose (3-OMG) and 100  $\mu$ mol/L 3-OMG in the presence or absence of 1 mmol/L phlorizin (SGLT1-inhibitor) and 10 mmol/L glucose. The reaction was stopped and the cells were washed twice with ice-cold Na-free buffer containing 25 mmol/L D-glucose. The cells were then processed as described above. SGLT1-specific uptake was calculated by subtracting uptake with and without phlorizin.

### Uptake studies in rabbit villus cell BBMV

Na<sup>+</sup>/H<sup>+</sup> exchange uptake was measured in BBMV by rapid-filtration technique as previously described (Manokas *et al.* 2000; Coon and Sundaram 2003; Coon *et al.* 2005). Briefly, 5  $\mu$ L of BBMV was suspended in 300 mmol/L mannitol, 50 mmol/L Tris-MES (pH 5.5) or 50 mmol/L Tris-HEPES (pH 7.5), and incubated in 95  $\mu$ L of reaction medium containing 300 mmol/L mannitol, 50 mmol/L Tris-HEPES (pH 7.5 at room temperature), 1 mmol/L <sup>22</sup>NaCl and with or without 1 mmol/L amiloride. At 60 sec, uptake was arrested by mixing with ice-cold stop solution (300 mmol/L mannitol, 50 mmol/L Tris-HEPES (pH 7.5)). The results were expressed as Na<sup>+</sup>/H<sup>+</sup> exchange uptake in picomoles per milligram protein at 60 sec. To derive kinetic parameters of BBM Na<sup>+</sup>/H<sup>+</sup> exchange, the numbers obtained from kinetic experiments were analyzed using GraphPad Prism 7 (San Diego, CA).

For Na-glucose cotransport uptake studies, BBMV uptake studies were performed by the rapid-filtration technique as previously described (Sundaram *et al.* 1997, 1998a; Turner and Black 2001). In brief, 5  $\mu$ L of BBMV was suspended in Na-free buffer containing 130 mmol/L TMACl, 4.7 mmol/L KCl, 1 mmol/L MgSO<sub>4</sub>, 1.25 mmol/L CaCl<sub>2</sub>, 20 mmol/L HEPES (pH 7.4). The BBMV was then incubated in 95  $\mu$ L of reaction medium that contained 130 mmol/L NaCl, 4.7 mmol/L KCl, 1 mmol/L MgSO<sub>4</sub>, 1.25 mmol/L CaCl<sub>2</sub>, 20 mmol/L HEPES (pH 7.4 at room temperature), 10  $\mu$ Ci of <sup>3</sup>H-O-methyl glucose (OMG), and 100  $\mu$ mol/L OMG in the presence or absence of 1 mmol/L phlorizin. At 90 sec, uptake was arrested by mixing with ice-cold stop solution (Na-free buffer) containing 25 mmol/L D-glucose. The uptake experiment results were expressed as Na-glucose cotransport uptake in nanomoles per milligram protein at 90 sec. To determine the kinetic parameters of BBM Na-glucose cotransport, the numbers obtained with kinetics

experiments were analyzed using GraphPad Prism 7 (San Diego, CA).

### Enzyme measurement

$\text{Na}^+/\text{K}^+$ -ATPase was measured as  $P_i$  liberated in GSNAP treated and untreated villus cells and IEC-18 cellular homogenates, as previously described (Forbush 1983; Palaniappan and Sundaram 2018). Enzyme-specific activity was expressed as nanomoles of  $P_i$  released per milligram protein per minute.

### Western blot analyses

Western blot analyses of villus cell and IEC-18 cell BBM were performed as described previously (Palaniappan and Sundaram 2018). BBM solubilized in RIPA buffer (50 mmol/L Tris HCl pH 7.4, 1% Igepal, 150 mmol/L NaCl, 1 mmol/L EDTA, 1 mmol/L PMSF, 1 mmol/L  $\text{Na}_3\text{VO}_4$ , 1 mmol/L NaF) containing protease inhibitor cocktail (SAFC Biosciences) was mixed with sample buffer (100 mmol/L Tris, 25% glycerol, 2% SDS, 0.01% bromophenol blue, 10% 2-ME, pH 6.8) and separated on a custom made 8% poly acrylamide gel. The separated proteins were transferred to BioTrace PVDF membrane and after blocked probed with anti-NHE3 antibodies and anti-SGLT1 antibodies raised in chicken (Invitrogen custom antibody services, USA) and anti-Ezrin antibodies (ab231907, Abcam, USA) raised in rabbit, at dilution of 1:1000 overnight at 4°C in fat-free milk containing 1× TBS-Tween 20. Horseradish peroxidase coupled rabbit antichick antibody (Prod # 31401, Invitrogen, USA) for NHE3 and SGLT1, goat antirabbit antibody (sc-2357, Santa Cruz, USA) for Ezrin at dilution of 1:10,000 for 1 h at room temperature in fat-free milk containing 1× TBS-Tween 20 were used to detect the binding of specific primary antibodies of both transporters. The resulting chemiluminescence with ECL Detection Reagent (GE Healthcare) was measured by autoradiography. NHE3 and SGLT1 protein density was quantitated via a densitometric scanner FluorChem™ instrument (Alpha Innotech, San Leandro, CA).

### Protein quantification

For all the uptake and molecular studies, proteins were quantified with the DC™ protein assay kit (Lowry's method) according to manufacturer's protocols (Bio-Rad).

### Statistical analysis

Results presented represent means  $\pm$  SE of experiments performed and calculated by the GraphPad Prism 7 (San Diego, CA). All uptakes were done in triplicate. Student's *t*-test was performed for statistical analysis.

## Results

### Effect of GSNAP on intracellular NO levels

The lowest possible dose of GSNAP that produced a reproducible increase in cNO was used in all experiments. In vivo treatment of rabbits with 500 nmol/L GSNAP modestly but significantly increased the intracellular cNO levels (Fig. 1a). Therefore, this concentration of GSNAP was used in all in vivo experiments. Similarly, when IEC-18 cells were treated with 250 nmol/L GSNAP, it increased the intracellular cNO to modest levels as well (Fig. 1b). This concentration of GSNAP was then used in all subsequent in vitro studies.

### Effect of GSNAP on $\text{Na}^+/\text{H}^+$ exchange in villus BBMV in vivo

In in vivo, GSNAP inhibited amiloride-sensitive  $^{22}\text{Na}$  uptake in villus cell BBMV prepared from control and GSNAP-treated rabbits (Fig. 2; control  $1043 \pm 62$  pmol/mg protein·min and GSNAP  $512.3 \pm 51.4$ ;  $n = 6$ ,  $P < 0.001$ ). These data demonstrated that the stimulation

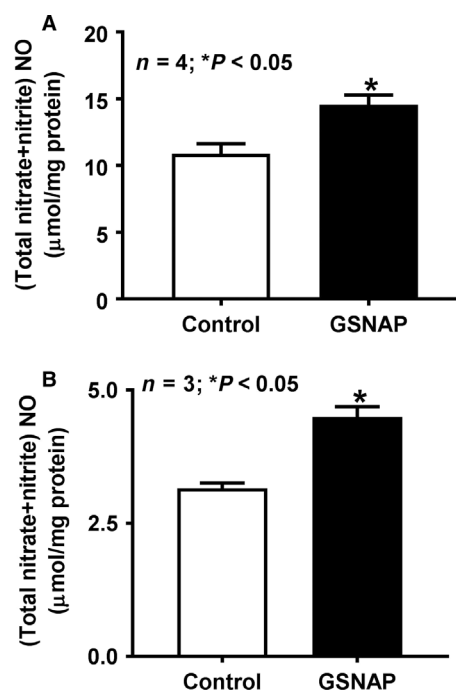


**Figure 1.** Effect of GSNAP on intracellular NO levels. (A) In vivo treatment with NO donor GSNAP in rabbits modestly, but significantly increased cNO levels in villus cells compared to control. (B) In vitro treatment of IEC-18 cells with GSNAP also increased intracellular cNO. Thus, in vivo or in vitro, GSNAP increased intracellular cNO in intestinal epithelial cells.

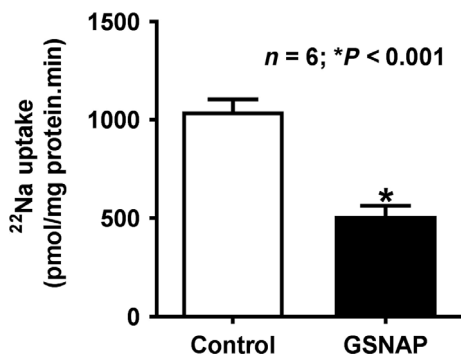


**Figure 2.** Effect of GSNAP on  $\text{Na}^+/\text{H}^+$  exchange in villus BBMVs. In GSNAP-treated rabbit villus BBMVs, proton gradient-dependent, amiloride-sensitive  $\text{Na}^+/\text{H}^+$  exchange was significantly diminished when compared with control villus BBMVs. Thus,  $\text{Na}^+/\text{H}^+$  exchange inhibition is due to increased cNO levels in rabbit villus cells.

of cNO production decreased  $\text{Na}^+/\text{H}^+$  exchange in the villus cell BBMVs.

### Effect of GSNAP on $\text{Na}^+/\text{H}^+$ exchange in IEC-18 cells

$\text{Na}^+/\text{H}^+$  exchange was significantly diminished in GSNAP-treated IEC-18 cells compared to control as shown in Figure 3 ( $1711 \pm 13.4$  pmol/mg protein-2 min in GSNAP-treated IEC-18 cells and  $2312 \pm 89$  in control;  $n = 4$ ,  $P < 0.001$ ). These data demonstrated that the stimulation of cNO production decreases BBM  $\text{Na}^+/\text{H}^+$  exchange in vitro in IEC-18 cells.

### Effect of GSNAP on Na-glucose cotransport in villus cell BBMVs in vivo

In in vivo, GSNAP treatment stimulated Na-dependent phlorizin-sensitive  $^3\text{H}$ -OMG uptake in villus cell BBMVs

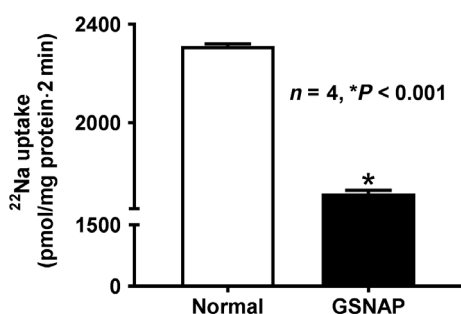


**Figure 3.** Effect of GSNAP on  $\text{Na}^+/\text{H}^+$  exchange in IEC-18 cells. Direct in vitro stimulation of cNO with GSNAP in IEC-18 significantly diminished proton gradient-dependent, EIPA-sensitive Na uptake when compared with control IEC-18 cells. These data indicated that an increased NO inhibited NHE3 in IEC-18 cells

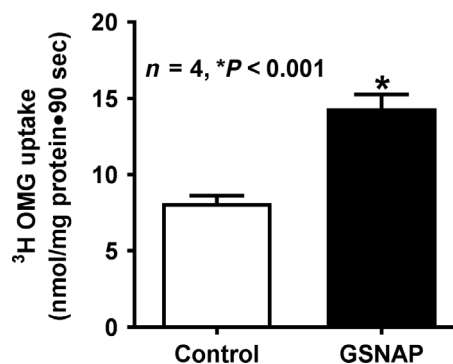


**Figure 4.** Effect of GSNAP on Na-glucose cotransport in villus cell BBMVs. In GSNAP-treated rabbit villus BBMVs, Na-dependent glucose cotransport ( $^3\text{H}$ -OMG uptake) was significantly increased when compared with control. Thus, Na-glucose cotransport stimulation is due to increased cNO levels in rabbit villus cells.

(Fig. 4; control  $8.1 \pm 0.5$  nmol/mg protein-90 sec and GSNAP  $14.4 \pm 0.9$ ;  $n = 4$ ,  $P < 0.001$ ). These data demonstrated that the stimulation of cNO production increases Na-glucose cotransport in the villus cell BBMVs.

### Effect of GSNAP on Na-glucose cotransport in IEC-18 cells

Na-glucose cotransport was significantly increased in GSNAP-treated IEC-18 cells compared to control (Fig. 5;  $1168 \pm 23.2$  pmol/mg protein-2 min in GSNAP-treated cells and  $745.9 \pm 9.8$  in control;  $n = 4$ ,  $P < 0.001$ ). These data demonstrated that the stimulation of cNO production increases BBM Na-glucose cotransport in vitro in IEC-18 cells.

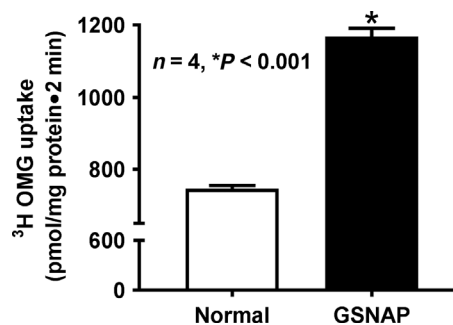


**Figure 5.** Effect of GSNAP on Na-glucose cotransport in IEC-18 cells. Direct in vitro stimulation of cNO with GSNAP in IEC-18 significantly increased Na-dependent and phlorizin-sensitive  $^3\text{H}$ -OMG uptake when compared with control IEC-18 cells. These data also indicated that intracellular increase in NO stimulated SGLT1 activity in IEC-18 cells.

### Effect of GSNAP on Na<sup>+</sup>/K<sup>+</sup>-ATPase activity

Since Na<sup>+</sup>/K<sup>+</sup>-ATPase in the basolateral membrane (BLM) provides the favorable Na gradient for SGLT1 in intact cells, its activity was determined in cellular homogenates from all experimental conditions. GSNAP treatment decreased Na<sup>+</sup>/K<sup>+</sup>-ATPase activity in IEC-18 cells ( $24.2 \pm 1.0$  nmol  $P_i$ /mg protein·min in control and GSNAP  $15.3 \pm 1.5$ ;  $n = 4$ ,  $P < 0.01$ ) and in villus cells (control  $14.8 \pm 0.7$  nmol  $P_i$ /mg protein·min and GSNAP  $11.6 \pm 0.5$ ;  $n = 6$ ,  $P < 0.05$ ). This indicated that the effect of GSNAP on Na-glucose cotransport was not secondary to enhanced transcellular Na gradient.

### Kinetic studies of NHE3 inhibition in rabbit villus cell BBMV and IEC-18 cells

Kinetic studies were performed to determine the mechanism of inhibition of Na<sup>+</sup>/H<sup>+</sup> exchange in the small intestine due to increased cNO. Uptake for all the concentrations was carried out at 6 sec since the initial rate of uptake for Na<sup>+</sup>/H<sup>+</sup> exchange in BBMV was linear for at least 10 sec. As the concentration of extra vesicular Na was increased, the uptake of <sup>22</sup>Na was stimulated and subsequently became saturated in all conditions (Fig. 6A). Table 1 shows the kinetic parameters derived from these experiments. The kinetic parameters demonstrated that the affinity [1/Michaelis constant ( $1/K_m$ )] for <sup>22</sup>Na uptake was not altered by the increase in cNO production (Table 1A). However, the maximal rate of uptake ( $V_{max}$ ) was significantly inhibited by GSNAP treatment (Table 1A). These data demonstrated that an increase in cNO production inhibits Na<sup>+</sup>/H<sup>+</sup> exchange in rabbit villus cells secondary to a decrease in the number of BBM exchangers rather than altered affinity of the exchangers for Na (Fig. 6A).

In IEC-18 cells, uptake for all the concentrations was carried out at 30 sec because the initial rate of uptake for Na<sup>+</sup>/H<sup>+</sup> exchange in IEC-18 cells was linear for at least 60 sec. As the concentration of extracellular Na was increased the uptake of <sup>22</sup>Na was stimulated and subsequently became saturated in all conditions (Fig. 6B). The  $K_m$  for Na was not altered in GSNAP-treated IEC-18 cells (Table 1B). However, the  $V_{max}$  was significantly decreased in IEC-18 cells treated with GSNAP (Table 1B). These data indicated that the mechanism of NHE3 inhibition by GSNAP in IEC-18 cells is also secondary to a decrease in the number of exchangers rather than a decrease in the affinity of the exchangers for Na.

### Kinetic studies of SGLT1 stimulation in rabbit villus cell BBMV and IEC-18 cells

Kinetic studies were performed to determine the mechanism of stimulation of Na-glucose cotransport in the

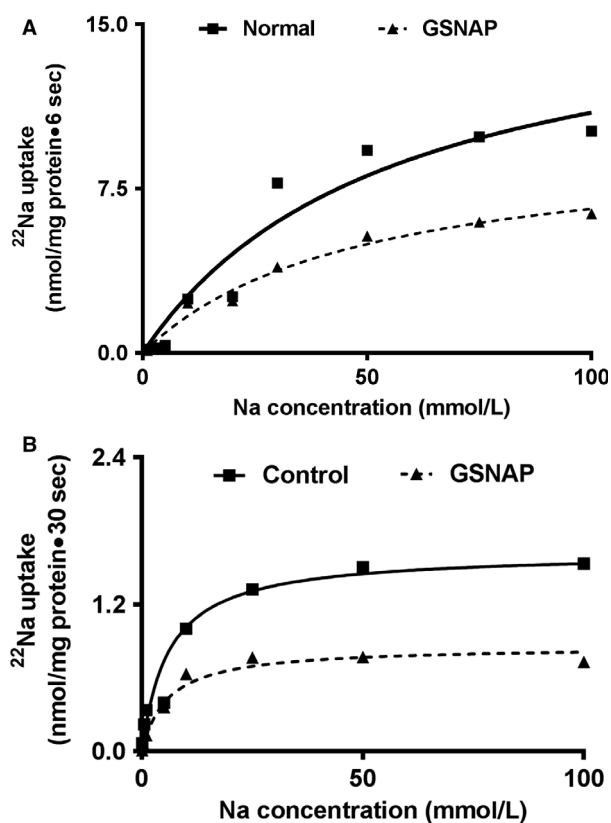


**Figure 6.** Kinetic studies of NHE3 inhibition in rabbit villus cell BBMV and IEC-18 cells. (A) In rabbit villus cell BBMV, as the extra vesicular Na concentration was increased, Na uptake was stimulated and then reached steady state. The kinetic parameters demonstrated that the affinity [1/Michaelis constant ( $1/K_m$ )] for <sup>22</sup>Na uptake was not altered by the increase in cNO production (Table 1A). However, the maximal rate of uptake ( $V_{max}$ ) was significantly inhibited by GSNAP treatment (Table 1A). (B) Similarly in IEC-18 cells, as the extracellular Na concentration was increased, Na uptake was stimulated and subsequently became saturated in all conditions. The kinetic parameters demonstrated that the affinity for <sup>22</sup>Na uptake was not altered by the increase in cNO production in IEC-18 cells (Table 1B). However, the maximal rate of uptake ( $V_{max}$ ) was significantly inhibited by GSNAP treatment in these cells (Table 1B).

small intestine due to increased cNO. Uptake for all the concentrations was carried out at 6 sec since the initial rate of uptake for Na-dependent glucose in BBMV was linear for at least 10 sec. As the concentration of extra vesicular Na was increased, the uptake of Na-dependent <sup>3</sup>H-OMG uptake was stimulated and subsequently became saturated in all conditions (Fig. 7A). Table 2A shows the kinetic parameters derived from these studies. The kinetic parameters demonstrated that the affinity for glucose was significantly stimulated by increased cNO. However, the  $V_{max}$  was not altered by GSNAP treatment (Table 2A). Thus, these data

**Table 1.** Kinetic parameters of Na<sup>+</sup>/H<sup>+</sup> exchange in rabbit villus BBMV and IEC-18 cells. (A) Rabbit villus cell BBMV: The maximal rate of uptake of sodium ( $V_{max}$ ) was significantly decreased in villus BBMV from GSNAP-treated rabbits; however, the affinity ( $1/K_m$ ) for sodium uptake was unaltered; (B) IEC-18 cells: The maximal rate of uptake of Na was also significantly decreased in GSNAP-treated IEC-18 cells. However, the affinity of the exchanger for Na was unchanged between control and GSNAP-treated IEC-18 cells.

| (A) NHE3 Kinetics – Villus cell BBMV |                                    |                |
|--------------------------------------|------------------------------------|----------------|
|                                      | $V_{max}$ (nmol/mg protein 6-sec)  | $K_m$ (mmol/L) |
| Control                              | 17.0 ± 2.2                         | 55.3 ± 0.7     |
| GSNAP                                | 9.7 ± 1.7*                         | 47.6 ± 7.2     |
| (B) NHE3 Kinetics – IEC-18 cells     |                                    |                |
|                                      | $V_{max}$ (nmol/mg protein 30-sec) | $K_m$ (mmol/L) |
| Control                              | 1.6 ± 0.1                          | 5.9 ± 0.7      |
| GSNAP                                | 0.8 ± 0.1*                         | 4.9 ± 0.5      |

\* $P < 0.01$ ,  $n = 3$ .

demonstrated that an increase in cNO production stimulated Na-glucose cotransport in rabbit villus cells secondary to an increase in the affinity of the cotransporter for glucose rather than an increase in the number of cotransporters (Fig. 7A).

In IEC-18 cells, uptake for all the concentrations was carried out at 30 sec because the initial rate of uptake for Na-dependent glucose cotransport in IEC-18 cells was linear for at least 60 sec. As the concentration of extravascular OMG was increased, the uptake of Na-dependent <sup>3</sup>H-OMG was stimulated and subsequently became saturated in all conditions (Fig. 7B). The kinetic parameters demonstrated that the affinity for <sup>3</sup>H-OMG uptake was significantly stimulated by increased cNO (Table 2B). However,  $V_{max}$  was not altered by GSNAP treatment (Table 2B). Thus, these data demonstrated that an increase in cNO production also stimulated Na-glucose cotransport in IEC-18 cells secondary to an increase in the affinity of the cotransporters for glucose rather than an increase in the number of BBM cotransporters.

### NHE3 molecular studies

Na<sup>+</sup>/H<sup>+</sup> exchange is mediated by NHE3 in the BBM of intestinal epithelial cells. Western blot analysis showed that the immunoreactive NHE3 protein levels in the villus cell BBM were significantly decreased in animals treated with GSNAP (Fig. 8A). Densitometric quantitation shown in Figure 8B, confirmed these findings. Immunoreactive NHE3 protein levels were also decreased in the BBM of IEC-18 cells by GSNAP treatment (Fig. 8C). Densitometric quantitation shown in Figure 8D, confirmed these

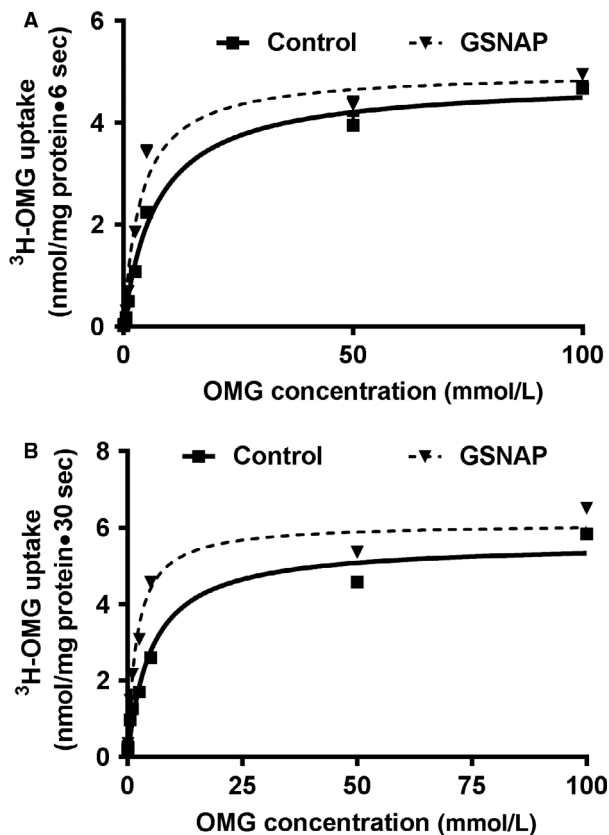


**Figure 7.** Kinetic studies of SGLT1 stimulation in rabbit villus cell BBMV and IEC-18 cells. (A) In rabbit villus cell BBMV, as the extravascular glucose concentration was increased, Na-dependent glucose uptake was stimulated and then reached steady state. The kinetic parameters demonstrated that the affinity for <sup>3</sup>H-OMG uptake was significantly stimulated by the increase in cNO (Table 2A). However, the maximal rate of uptake was not altered by GSNAP treatment (Table 2A). (B) Comparably in IEC-18 cells, as the extracellular glucose concentration was increased, glucose uptake was stimulated and subsequently became saturated in all conditions. The kinetic parameters demonstrated that the affinity for <sup>3</sup>H-OMG uptake was significantly stimulated by the increase in cNO in IEC-18 cells as well (Table 2B). However, the maximal rate of uptake was not altered by GSNAP treatment in these cells (Table 2B).

findings. The decrease in NHE3 protein in conjunction with kinetic studies demonstrated that the mechanism of inhibition of NHE3 is secondary to a decrease in the number of BBM exchangers rather than a decrease in the affinity of the exchangers for Na.

### SGLT1 molecular studies

As shown in Figure 9A, Western blot analyses demonstrated that GSNAP treatment did not affect SGLT1 immunoreactive protein levels in rabbit villus cell BBM

**Table 2.** Kinetic parameters of Na-glucose co-transport in rabbit villus BBMV and IEC-18 cells. (A) Rabbit villus cell BBMV: The maximal rate of uptake of glucose was not affected in villus BBMV from GSNAP-treated rabbits; however, the affinity for glucose uptake was significantly increased in GSNAP-treated rabbits. (B) IEC-18 cells: The affinity for glucose was also significantly increased in GSNAP-treated IEC-18 cells. However, the maximal rate of uptake of glucose was unchanged between control and GSNAP-treated IEC-18 cells.

| (A) SGLT1 Kinetics – Villus cell BBMV |                                    |                |
|---------------------------------------|------------------------------------|----------------|
|                                       | $V_{max}$ (nmol/mg protein·6 sec)  | $K_m$ (mmol/L) |
| Control                               | 4.8 ± 0.1                          | 7.2 ± 0.6      |
| GSNAP                                 | 5.0 ± 0.1                          | 3.8 ± 0.3*     |
| (B) SGLT1 kinetics – IEC-18 cells     |                                    |                |
|                                       | $V_{max}$ (nmol/mg protein·30 sec) | $K_m$ (mmol/L) |
| Control                               | 5.6 ± 0.3                          | 5.2 ± 0.2      |
| GSNAP                                 | 6.1 ± 0.1                          | 1.9 ± 0.1*     |

\* $P < 0.01$ ;  $n = 6$ .

\* $P < 0.01$ ;  $n = 4$ .

(Fig. 9B). Western blot analysis also showed that GSNAP treatment did not affect SGLT1 immunoreactive protein levels in IEC-18 cell BBM (Fig. 9C). Densitometric quantitation shown in Figure 9D confirmed the findings. In conjunction with kinetic studies, these molecular studies demonstrated that the mechanism of stimulation of SGLT1 is secondary to an increase in the affinity of the cotransporter for glucose rather than an increase in the number of cotransporters in the BBM.

## Discussion

This study demonstrates that a moderate increase in cNO stimulated SGLT1 in vivo in rabbit intestinal villus cells and in vitro in IEC-18 cells. In contrast, an elevation in cNO inhibited NHE3 in vivo in rabbit intestinal villus cells and in vitro in IEC-18 cells. The mechanism of stimulation of SGLT1 was secondary to enhanced affinity of the cotransporter for glucose without a change in the number of BBM cotransporters. Whereas, the mechanism of inhibition of NHE3 was secondary to an increase in the number of exchangers in the BBM without a change in the affinity of the exchanger for Na. Thus, it is likely that cNO uniquely and possibly compensatorily regulates the primary Na absorptive pathways in the mammalian small intestine to maintain cellular Na homeostasis.

This study illustrates that moderate increase in cNO in vivo increases intestinal glucose absorption by stimulating SGLT1 in villus cells. These findings are diametrically opposite to those seen when cNO production was reduced in vivo with L-NAME in rabbits. This resulted in

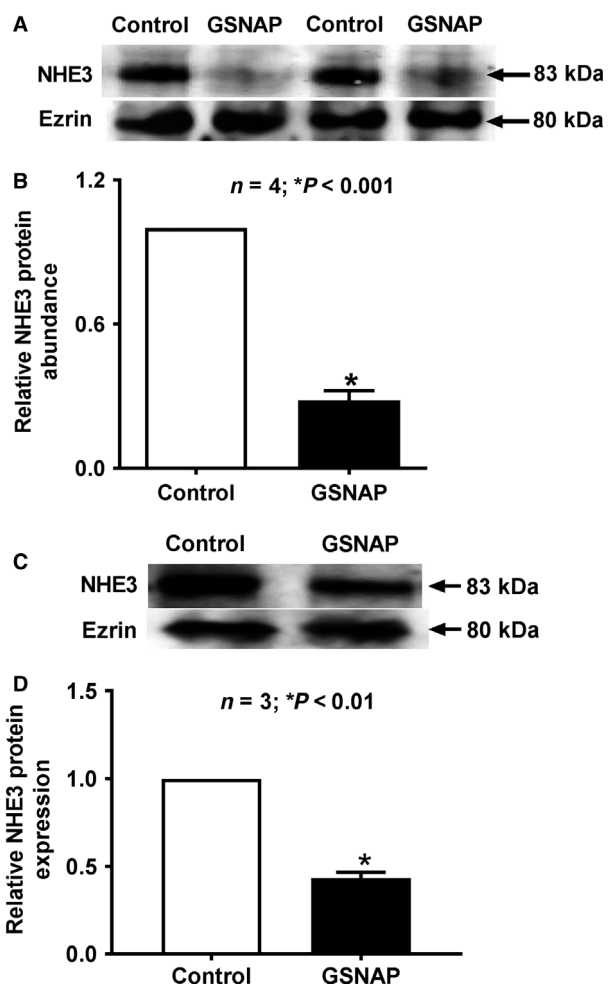


**Figure 8.** NHE3 molecular studies – effect of GSNAP on villus cell BBM NHE3 protein expression. (A) Representative Western blot shows that in GSNAP-treated BBM of rabbit villus cells there is reduction of NHE3 protein expression compared with control villus cell BBM. (B) Densitometry quantitation confirmed that treatment with GSNAP significantly decreased BBM NHE3 levels in villus cells. (C) Similarly in IEC-18 cells, increased cNO significantly downregulated BBM NHE3 protein expression compared with control IEC-18 cells. (D) Densitometry quantitation confirmed that treatment with GSNAP significantly decreased BBM NHE3 levels in IEC-18 cells as well.

inhibition of SGLT1 secondary to diminished affinity of the cotransporter for glucose without a change in the number of BBM cotransporters (Coon et al. 2005). The kinetic parameters are comparable for control villus cells in both studies, with increased affinity when cNO is increased as shown in this study, while  $K_m$  was decreased when cNO was inhibited as previously shown (Coon et al. 2005). Thus, an increase in intracellular cNO stimulates SGLT1 while a decrease in cNO inhibits SGLT1 in mammalian intestinal villus cells.



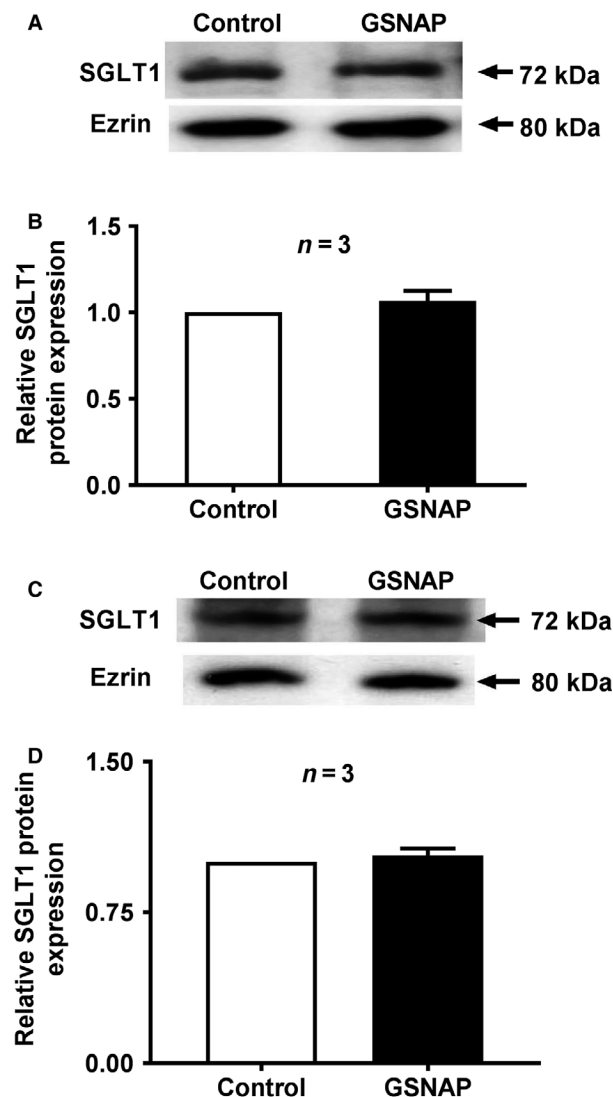


**Figure 9.** SGLT1 molecular studies – effect of GSNAP on villus cell BBM SGLT1 protein expression. (A) Representative Western blot shows that in GSNAP-treated BBM of rabbit villus cells there is no change in SGLT1 protein expression compared with control villus cell BBM. (B) Densitometry quantitation confirmed that treatment with GSNAP did not affect BBM SGLT1 levels in villus cells. (C) Similarly in IEC-18 cells, increased cNO did not affect BBM SGLT1 protein expression compared with control BBM of IEC-18 cells. (D) Densitometry quantitation confirmed that treatment with GSNAP did not alter BBM SGLT1 levels in IEC-18 cells as well.

In vivo cNO inhibition may have multiple other effects, which may in turn affect SGLT1 activity. Therefore, in vitro studies in IEC-18 cells were performed to determine cNO increase mediated specific alterations in SGLT1 activity. Enhanced intracellular cNO also increased SGLT1 activity in IEC-18 cells. The mechanism of stimulation of SGLT1 was secondary to enhanced affinity of the

cotransporter for glucose without a change in the maximal rate of uptake of glucose. Consistent with this, molecular studies did not show any change in the BBM immunoreactive levels of SGLT1. These findings were identical to the in vivo observations in rabbits when cNO was increased. However, these findings are completely opposite to those demonstrated when cNO production was directly reduced in vitro in IEC-18 cells. Direct inhibition of cNO in IEC-18 cells resulted in inhibition of SGLT1 secondary to a decrease in the affinity of the cotransporter for glucose without a change in the number of BBM cotransporters (Coon et al. 2008; Palaniappan and Sundaram 2018). In IEC-18 cells while the  $K_m$  for control in the current and prior studies were comparable, it was shown to be substantially decreased in the prior study when cNO was diminished (Coon et al. 2008) and in this study  $K_m$  was significantly increased when cNO is enhanced. Thus, whether in vivo or in vitro, in two different species, when cNO is increased or decreased it subsequently stimulated or inhibited SGLT1, respectively, by exactly the same mechanism, specifically by altering the affinity of the cotransporter for glucose. As mentioned before, the primary glucose absorption in mammalian intestine is via SGLT1. Therefore, alteration of SGLT1 activity by cNO levels could be central to the altered glucose homeostasis and pathophysiology of diabetes, which affects almost ten percent of the American population (Selvin and Ali 2017).

A recent study showed that NO is a significant player in the pathology of gestational diabetes (Usman et al. 2018). Another study has established that systemic glucose metabolism is modulated through enteric nitric oxide synthase (Abot et al. 2018). Moreover, NO was found to be the regulator of glucose utilization in gut-brain axis (Fournel et al. 2017). In this context, this study establishes that NO through the regulation of SGLT1 in the intestine may modulate glucose homeostasis and therefore may be involved in the pathology of diabetes.

Whether in vivo or in vitro, the stimulation of SGLT1 is not secondary to altered Na-extruding capacity of the cell although  $\text{Na}^+/\text{K}^+$ -ATPase was decreased. Since the mechanism of stimulation of SGLT1 was secondary to enhanced affinity of the cotransporter for glucose, cNO appears to modulate SGLT1 at the posttranslational level by affecting the affinity of the cotransporter for glucose. Altered affinity may be secondary to altered phosphorylation and or glycosylation of the cotransporter. In a prior study, it was demonstrated that when cNO production was inhibited, it reduced intracellular cGMP, and via protein kinase G increased the glycosylation of SGLT1 which resulted in the inhibition of its activity (Arthur et al. 2014). The intracellular pathway responsible for the

increase in affinity resulting in the stimulation of SGLT1 by increased cNO is yet to be determined.

Apart from altering glucose homeostasis, stimulation of SGLT1 by enhanced cNO will also alter Na homeostasis. Perhaps to compensate for this intracellular Na imbalance, in cNO stimulated cells, the other primary Na absorptive pathway, namely NHE3, appears to be inhibited. This observation is pertinent to conditions associated with deregulated Na absorption such as hypertension. Based on most recent guidelines, 46% of U.S. adults, about 103 million, have hypertension (Fryar *et al.* 2017; Whelton *et al.* 2018). Numerous randomized trials and observational studies have demonstrated a direct relationship between assimilation of dietary sodium and blood pressure (Aburto *et al.* 2013; He *et al.* 2013). Furthermore, there is a consistent effect of lowering sodium assimilation on blood pressure among those with hypertension (Whelton *et al.* 1998; Sacks *et al.* 2001). A recent Cochrane meta-analysis of data from 35 trials (He *et al.* 2013) found that a 100 mmol reduction in 24-h urinary sodium led to a significant reduction in systolic/diastolic blood pressure of 5.4/2.8 mm Hg among hypertensive individuals. Finally, studies have demonstrated an increased risk of mortality for high-sodium assimilation and a direct relationship with total mortality, even at the lowest levels of sodium intake (Cook *et al.* 2016).

In vivo stimulation of intracellular cNO inhibits NHE3 activity in villus cells. The mechanism of inhibition is secondary to a decrease in the number of exchangers in the BBM of villus cells without an alteration in the affinity of the exchanger for Na. These findings are also diametrically opposite to those demonstrated when cNO production was reduced in vivo in rabbits. This resulted in the stimulation of villus cell NHE3 activity. The mechanism of stimulation of NHE3 was secondary to enhanced transporter numbers in the BBM without a change in the affinity of the exchanger for Na (Coon *et al.* 2007). The kinetic parameters are comparable for control villus cells in both studies, with diminished  $V_{max}$  when cNO is increased as shown in this study, whereas  $V_{max}$  was increased when cNO was decreased as previously shown (Coon *et al.* 2007). Finally, possible mechanisms of stimulation of NHE3 include increased de novo synthesis of protein, enhanced trafficking to BBM and/or enhanced mRNA stability of NHE3 transcription. Thus, unlike SGLT1, an increase in intracellular cNO inhibits NHE3 while a decrease in cNO stimulates NHE3 in mammalian intestinal villus cells.

To avoid untoward complications of in vivo increases in cNO, in this study in vitro direct stimulation of intracellular cNO at physiological levels was done which produced results opposite that noted above. Specifically,

increased cNO inhibited NHE3 in IEC-18 cells. The mechanism of inhibition was secondary to decreased BBM transporter numbers. This effect was also seen in human colon cancer Caco2 cells (Gill *et al.* 2002). In contrast, when cNO was directly inhibited in IEC-18 cells, it stimulated NHE3 in these cells by increasing the BBM exchanger numbers. Kinetic studies in prior and current study are consistent with this. In IEC-18 cells while the  $V_{max}$  for control in the current and prior studies were comparable, it was shown to be substantially increased in the prior study when cNO was diminished and in this study  $V_{max}$  was significantly decreased when cNO is enhanced (Coon *et al.* 2008). Thus, when cNO is increased or decreased, it subsequently inhibits NHE3 or stimulates NHE3 by exactly the same mechanism, by altering BBM transporter numbers.

In contrast to SGLT1, the mechanism of inhibition of villus cell NHE3 by increased cNO is secondary to a decrease in exchanger numbers. The decrease in BBM NHE3 may be at the transcriptional level. Transcriptional regulation of NHE3 may occur at three levels: (1) diminished de novo NHE3 mRNA synthesis, (2) reduced NHE3 mRNA stability and/or (3) NHE3 promoter regulation; the sequence of rat NHE3 core promoter region between nucleotides -118 to +59 contains the essential transcription factor interacting sites of Sp 1 family members as well as AP1/CREB (Kiela *et al.* 2006). Alternatively, since a percentage of NHE3 is in the cytosol at baseline, altered cytosol to membrane trafficking may be the cause of enhanced transporter numbers in the BBM.

The concept of the two primary Na absorptive pathways in the intestine being compensatorily regulated to maintain Na homeostasis by cNO is consistent with the observation that NHE3 and SGLT1 do indeed regulate one another. When NHE3 was silenced in IEC-18 monolayers with NHE3 siRNA, the cells demonstrated decreased NHE3 activity, mRNA and protein. However, in NHE3 silenced cells, SGLT1 activity, mRNA, and protein in the BBM were significantly increased. Thus, inhibition of NHE3 expression compensatorily increased the expression and function of SGLT1 and vice versa in the BBM of intestinal epithelial cells. Thus, this study demonstrate that the major Na absorptive pathways function compensatorily to regulate Na absorption in intestinal epithelial cells.

This study, for the first time, demonstrates that an increase in intracellular cNO that is not pathological, compensatorily stimulates SGLT1 while inhibiting NHE3 in intestinal epithelial cells from rabbits and rats, in vivo and in vitro, respectively. Therefore, cNO directly, broadly and uniquely regulates intestinal epithelial cell BBM Na absorption by compensatorily regulating NHE3 and SGLT1.

## Conflict of Interest

No conflicts of interest, financial or otherwise, are declared by the authors.

## References

- Abot, A., A. Lucas, T. Bautzova, A. Bessac, A. Fournel, S. Le-Gonidec, et al. 2018. Galanin enhances systemic glucose metabolism through enteric Nitric Oxide Synthase-expressed neurons. *Mol. Metab.* 10:100–108.
- Aburto, N. J., A. Ziolkovska, L. Hooper, P. Elliott, F. P. Cappuccio, and J. J. Meerpohl. 2013. Effect of lower sodium intake on health: systematic review and meta-analyses. *BMJ* 346:f1326.
- Arthur, S., S. Coon, R. Kekuda, and U. Sundaram. 2014. Regulation of sodium glucose co-transporter SGLT1 through altered glycosylation in the intestinal epithelial cells. *Biochim. Biophys. Acta* 1838:1208–1214.
- Barry, M. K., J. D. Aloisi, S. P. Pickering, and C. J. Yeo. 1994. Nitric oxide modulates water and electrolyte transport in the ileum. *Ann. Surg.* 219:382.
- Cook, N. R., L. J. Appel, and P. K. Whelton. 2016. Sodium intake and all-cause mortality over 20 years in the trials of hypertension prevention. *J. Am. Coll. Cardiol.* 68:1609–1617.
- Coon, S., and U. Sundaram. 2003. Unique regulation of anion/HCO<sub>3</sub><sup>-</sup> exchangers by constitutive nitric oxide in rabbit small intestine. *Am. J. Physiol. Gastrointest. Liver Physiol.* 285:G1084–G1090.
- Coon, S., J. Kim, G. Shao, and U. Sundaram. 2005. Na-glucose and Na-neutral amino acid cotransport are uniquely regulated by constitutive nitric oxide in rabbit small intestinal villus cells. *Am. J. Physiol. Gastrointest. Liver Physiol.* 289:G1030–G1035.
- Coon, S., G. Shao, S. Wisel, R. Vulaupalli, and U. Sundaram. 2007. Mechanism of regulation of rabbit intestinal villus cell brush border membrane Na/H exchange by nitric oxide. *Am. J. Physiol. Gastrointest. Liver Physiol.* 292:G475–G481.
- Coon, S., R. Kekuda, P. Saha, J. R. Talukder, and U. Sundaram. 2008. Constitutive nitric oxide differentially regulates Na-H and Na-glucose cotransport in intestinal epithelial cells. *Am. J. Physiol. Gastrointest. Liver Physiol.* 294:G1369–G1375.
- De La Horra, M. C., M. Cano, M. J. Peral, M. L. Calonge, and A. A. Ilundáin. 2001. Hormonal regulation of chicken intestinal NHE and SGLT-1 activities. *Am. J. Physiol. Regul. Integr. Comp. Physiol.* 280:R655–R660.
- Donowitz, M., B. Cha, N. C. Zachos, C. L. Brett, A. Sharma, C. M. Tse, et al. 2005. NHERF family and NHE3 regulation. *J. Physiol.* 567:3–11.
- Forbush, B. 3rd. 1983. Assay of Na, K-ATPase in plasma membrane preparations: increasing the permeability of membrane vesicles using sodium dodecyl sulfate buffered with bovine serum albumin. *Anal. Biochem.* 128:159–163.
- Fournel, A., A. Drougard, T. Duparc, A. Marlin, S. M. Brierley, J. Castro, et al. 2017. Apelin targets gut contraction to control glucose metabolism via the brain. *Gut* 66:258–269.
- Fryar, C. D., Y. Ostchega, C. M. Hales, G. Zhang, and D. Kruszon-Moran. 2017. Hypertension prevalence and control among adults: United States, 2015–2016. *NCHS Data Brief* 289:1–8.
- Gill, R. K., S. Saksena, I. A. Syed, S. Tyagi, W. A. Alrefai, J. Malakooti, et al. 2002. Regulation of NHE3 by nitric oxide in Caco-2 cells. *Am. J. Physiol. Gastrointest. Liver Physiol.* 283:G747–G756.
- Grisham, M. B., K. P. Pavlick, F. S. Laroux, J. Hoffman, S. Bharwani, and R. E. Wolf. 2002. Nitric oxide and chronic gut inflammation: controversies in inflammatory bowel disease. *J. Invest. Med.* 50:272–283.
- Grundy, D. 2015. Principles and standards for reporting animal experiments in *The Journal of Physiology and Experimental Physiology*. *J. Physiol.* 593:2547–2549.
- He, F. J., J. Li, and G. A. MacGregor. 2013. Effect of longer term modest salt reduction on blood pressure: cochrane systematic review and meta-analysis of randomised trials. *BMJ* 346:f1325.
- Hoogerwerf, W. A., S. C. Tsao, O. Devuyst, S. A. Levine, C. H. Yun, J. W. Yip, et al. 1996. NHE2 and NHE3 are human and rabbit intestinal brush-border proteins. *Am. J. Physiol. Gastrointest. Liver Physiol.* 270:G29–G41.
- Kiela, P. R., H. Xu, and F. K. Ghishan. 2006. Apical Na<sup>+</sup>/H<sup>+</sup> exchangers in the mammalian gastrointestinal tract. *J. Physiol. Pharmacol.* 57:51–79.
- Kubes, P., and D.-M. McCafferty. 2000. Nitric oxide and intestinal inflammation. *Am. J. Med.* 109:150–158.
- MacNaughton, W. K. 1993. Nitric oxide-donating compounds stimulate electrolyte transport in the guinea pig intestine in vitro. *Life Sci.* 53:585–593.
- Manokas, T., J. J. Fromkes, and U. Sundaram. 2000. Effect of chronic inflammation on ileal short-chain fatty acid/bicarbonate exchange. *Am. J. Physiol. Gastrointest. Liver Physiol.* 278:G585–G590.
- Mourad, F., K. Barada, N. Abdel-Malak, N. Rached, C. Khoury, N. Saade, et al. 2003. Interplay between nitric oxide and vasoactive intestinal polypeptide in inducing fluid secretion in rat jejunum. *J. Physiol.* 550:863–871.
- Palaniappan, B., and U. Sundaram. 2018. Direct and specific inhibition of constitutive nitric oxide synthase uniquely regulates brush border membrane Na- absorptive pathways in intestinal epithelial cells. *Nitric Oxide* 79:8–13.
- Sacks, F. M., L. P. Svetkey, W. M. Vollmer, L. J. Appel, G. A. Bray, D. Harsha, et al. 2001. Effects on blood pressure of reduced dietary sodium and the Dietary Approaches to Stop Hypertension (DASH) diet. *N. Engl. J. Med.* 344:3–10.
- Saha, P., S. Arthur, R. Kekuda, and U. Sundaram. 2012. Na-glutamine co-transporters B 0 AT1 in villus and SN2 in crypts are differentially altered in chronically inflamed

- rabbit intestine. *Biochim. Biophys. Acta Biomembr.* 1818:434–442.
- Schirgi-Degen, A., and E. Beubler. 1998. Proabsorptive properties of nitric oxide. *Digestion* 59:400–403.
- Selvin, E., and M. K. Ali. 2017. Declines in the incidence of diabetes in the US—real progress or artifact? *Diabetes Care* 40:1139–1143.
- Shah, V., G. Lyford, G. Gores, and G. Farrugia. 2004. Nitric oxide in gastrointestinal health and disease. *Gastroenterology* 126:903–913.
- Stack, W., B. Filipowicz, and C. Hawkey. 1996. Nitric oxide donating compounds stimulate human colonic ion transport in vitro. *Gut* 39:93–99.
- Sundaram, U., and A. B. West. 1997. Effect of chronic inflammation on electrolyte transport in rabbit ileal villus and crypt cells. *Am. J. Physiol.* 272:G732–G741.
- Sundaram, U., R. G. Knickelbein, and J. W. Dobbins. 1991. pH regulation in ileum: Na(+)-H<sup>+</sup> and Cl(-)-HCO<sub>3</sub><sup>-</sup> exchange in isolated crypt and villus cells. *Am. J. Physiol.* 260:G440–G449.
- Sundaram, U., S. Wisel, V. M. Rajendren, and A. B. West. 1997. Mechanism of inhibition of Na<sup>+</sup>-glucose cotransport in the chronically inflamed rabbit ileum. *Am. J. Physiol.* 273:G913–G919.
- Sundaram, U., S. Wisel, and J. J. Fromkes. 1998a. Unique mechanism of inhibition of Na<sup>+</sup>-amino acid cotransport during chronic ileal inflammation. *Am. J. Physiol.* 275: G483–G489.
- Sundaram, U., S. Wisel, S. Stengelin, W. Kramer, and V. Rajendran. 1998b. Mechanism of inhibition of Na<sup>+</sup>-bile acid cotransport during chronic ileal inflammation in rabbits. *Am. J. Physiol. Gastrointest. Liver Physiol.* 275:G1259–G1265.
- Sundaram, U., S. Coon, S. Wisel, and A. B. West. 1999. Corticosteroids reverse the inhibition of Na-glucose cotransport in the chronically inflamed rabbit ileum. *Am. J. Physiol.* 276:G211–G218.
- Tamai, H., and T. S. Gaginella. 1993. Direct evidence for nitric oxide stimulation of electrolyte secretion in the rat colon. *Free Radical Res. Commun.* 19:229–239.
- Turner, J. R., and E. D. Black. 2001. NHE3-dependent cytoplasmic alkalinization is triggered by Na(+)-glucose cotransport in intestinal epithelia. *Am. J. Physiol. Cell Physiol.* 281:C1533–C1541.
- Turvill, J., F. Mourad, and M. Farthing. 1999. Proabsorptive and prosecretory roles for nitric oxide in cholera toxin induced secretion. *Gut* 44:33–39.
- Usman, T. O., E. D. Areola, O. O. Badmus, I. Kim, and L. A. Olatunji. 2018. Sodium acetate and androgen receptor blockade improve gestational androgen excess-induced deteriorated glucose homeostasis and antioxidant defenses in rats: roles of adenosine deaminase and xanthine oxidase activities. *J. Nutr. Biochem.* 62:65–75.
- Whelton, P. K., L. J. Appel, M. A. Espeland, W. B. Applegate, W. H. Jr Ettinger, J. B. Kostis, et al. 1998. Sodium reduction and weight loss in the treatment of hypertension in older persons: a randomized controlled trial of nonpharmacologic interventions in the elderly (TONE). *JAMA* 279:839–846.
- Whelton, P. K., R. M. Carey, W. S. Aronow, D. E. Casey, K. J. Collins, C. D. Himmelfarb, et al. 2018. 2017ACC/AHA/AAPA/ABC/ACPM/AGS/APhA/ASH/ASPC/NMA/PCNA guideline for the prevention, detection, evaluation, and management of high blood pressure in adults: a report of the American College of Cardiology/American Heart Association Task Force on Clinical Practice Guidelines. *J. Am. Coll. Cardiol.* 71:e127–e248.
- Wright, E., D. Loo, B. Hirayama, and E. Turk. 2006. Sugar absorption. Pp. 1653–1665 *in* L. Johnson, K. Barrett, F. Ghishan, J. Merchant, H. Said and J. Wood, eds. *Physiology of gastrointestinal tract*, 4th edn. Academic, Baltimore.
- Wright, E. M., B. A. Hirayama, and D. F. Loo. 2007. Active sugar transport in health and disease. *J. Intern. Med.* 261:32–43.